arXiv:1704.03459v1 [stat.CO] 11 Apr 2017

Bayesian Analysis (0000) **00**, Number 0, pp. 1

Dynamic nested sampling: an improved algorithm for parameter estimation and evidence calculation

Edward Higson[*,¶,‖], Will Handley[†,¶,‖], Mike Hobson[‡,¶] and Anthony Lasenby[§,¶,‖]

Abstract. We introduce dynamic nested sampling: a generalisation of the nested sampling algorithm in which the number of "live points" varies to allocate samples more efficiently. In empirical tests the new method increases accuracy by up to a factor of ~8 for parameter estimation and ~3 for evidence calculation compared to standard nested sampling with the same number of samples — equivalent to speeding up the computation by factors of ~64 and ~9 respectively. In addition unlike in standard nested sampling more accurate results can be obtained by continuing the calculation for longer. Dynamic nested sampling can be easily included in existing nested sampling software such as MultiNest and PolyChord.

Keywords: nested sampling, parameter estimation, Bayesian evidence.

1 Introduction

Nested sampling (Skilling, 2006) is a Monte Carlo method for Bayesian analysis which simultaneously calculates Bayesian evidences and posterior samples. Initial development of the algorithm focused on evidence calculation, but implementations such as MultiNest (Feroz and Hobson, 2008; Feroz et al., 2009, 2013) and PolyChord (Handley et al., 2015a,b) are now also extensively used for parameter estimation from posterior samples (see for example Planck Collaboration (2016)).

Nested sampling exponentially compresses the prior distribution to the posterior by requiring samples have increasing likelihoods. Conventionally a fixed number of "live points" is used — we term this *standard nested sampling*. In this case the expected fractional shrinkage of the prior volume remaining is the same at each step, and as a result many samples are typically taken from regions of the prior that are remote from the bulk of the posterior. The allocation of samples in standard nested sampling is set by the likelihood and the prior, and cannot be changed depending on whether calculating the evidence or obtaining posterior samples is the primary goal.

We propose modifying the nested sampling algorithm by dynamically varying the

[*]e.higson@mrao.cam.ac.uk
[†]wh260@mrao.cam.ac.uk
[‡]mph@mrao.cam.ac.uk
[§]a.n.lasenby@mrao.cam.ac.uk
[¶]Astrophysics Group, Battcock Centre, Cavendish Laboratory, JJ Thomson Avenue, Cambridge CB3 0HE, UK
[‖]Kavli Institute for Cosmology, Madingley Road, Cambridge, CB3 0HA, UK

© 0000 International Society for Bayesian Analysis DOI: 0000

number of "live points" in order to maximise the accuracy of a calculation for some number of posterior samples, subject to practical constraints. We term this more general approach *dynamic nested sampling*, with standard nested sampling representing the special case where the number of live points is constant. Dynamic nested sampling is particularly effective for parameter estimation, as standard nested sampling typically spends most of its computational effort iterating towards the posterior peak. This produces posterior samples with negligible weights which make little contribution to the calculation's accuracy, as discussed in our previous analysis of sampling errors in nested sampling parameter estimation (Higson et al., 2017). We also achieve significant improvements in the accuracy of evidence calculations, and show both evidence and parameter estimates can be improved simultaneously.

Our approach can be easily incorporated into existing standard nesting sampling software such as MultiNest and PolyChord; we are currently working on its inclusion in the forthcoming PolyChord 2 package. This is in contrast to alternatives such as diffusive nested sampling (Brewer et al., 2011) and superposition enhanced nested sampling (Martiniani et al., 2014) which require additional software

The paper proceeds as follows: Section 2 contains background on nested sampling, and Section 3 establishes useful results about the effects of varying the number of live points. Our dynamic nested sampling algorithm for increasing efficiency for general nested sampling calculations is presented in Section 4; its accurate allocation of live points for a priori unknown posterior distributions is illustrated in Figure 5. Numerical tests of dynamic nested sampling's efficiency improvements over standard nested sampling are given in Section 5, which includes a discussion of the effects of likelihood, priors and dimensionality. In particular we find large efficiency gains for high-dimensional parameter estimation problems. In the manner described by Keeton (2011) we use analytical cases where one can obtain uncorrelated samples from the prior space within some likelihood contour using standard techniques, and we term the resulting procedure *perfect nested sampling* (in both standard and dynamic versions). We discuss including dynamic nested sampling in nested sampling software for practical problems in Section 6.

2 Background: the nested sampling algorithm

Nested sampling (Skilling, 2006) is a numerical method for computing Bayesian evidences

$$\mathcal{Z} = \int \mathcal{L}(\theta)\pi(\theta)\,\mathrm{d}\theta \tag{1}$$

and samples from the posterior distribution

$$\mathcal{P}(\theta) = \frac{\mathcal{L}(\theta)\pi(\theta)}{\mathcal{Z}} \tag{2}$$

given some likelihood $\mathcal{L}(\theta)$ and prior $\pi(\theta)$.

Initially some number of *live points* are sampled randomly from the prior π. In standard nested sampling, at each iteration i the point with the lowest likelihood $\mathcal{L}_i$

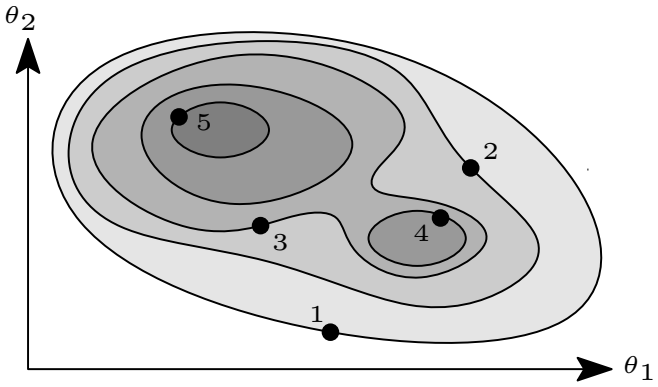

Figure 1: Nested sampling dead points and iso-likelihood contours for a two-dimensional multi-modal likelihood $\mathcal{L}(\theta)$; darker shading shows higher likelihoods.

is removed and replaced by a new live point sampled from the prior subject to the constraint that it has a likelihood higher than $\mathcal{L}_i$, as shown in Figure 1. As a result the number of live points remains constant throughout the process. Iterating until some termination condition is met generates a list of discarded samples (termed *dead points*), which are used to estimate the evidence and make posterior inferences[1]. We refer to the completed nested sampling process as a *run*.

To compute the evidence, the many-dimensional integral (1) is reduced to a one-dimensional integral in terms of the fractional prior volume within an iso-likelihood contour. We define the fraction of the prior θ with likelihood greater than some value $\mathcal{L}$ as $X(\mathcal{L})$, where

$$X(\mathcal{L}) \equiv \int_{\mathcal{L}(\theta)>\mathcal{L}} \pi(\theta)\,\mathrm{d}\theta, \tag{3}$$

and $X \in [0,1]$. Provided the inverse $\mathcal{L}(X) \equiv X^{-1}(\mathcal{L})$ exists[2], the evidence (1) can be expressed as

$$\mathcal{Z} = \int_0^1 \mathcal{L}(X)\,\mathrm{d}X. \tag{4}$$

Given a set of dead points with likelihoods $\mathcal{L}_i$, the corresponding prior volumes X_i are unknown but are modelled statistically as $X_i = t_i X_{i-1}$, where $X_0 = 1$. For a given number of live points n each shrinkage ratio t_i is independently distributed as the largest of n random variables from the interval $[0,1]$ (Skilling, 2006). Hence:

$$P(t_i) = n t_i^{n-1}, \qquad \mathrm{E}[\log t_i] = -\frac{1}{n}, \qquad \mathrm{Var}[\log t_i] = \frac{1}{n^2}, \tag{5}$$

and the algorithm samples within an exponentially shrinking part of the prior. In standard nested sampling the number of live points n is some constant value for all t_i — the iteration of the algorithm in this case is illustrated schematically in Figure 2.

[1] The remaining live points at termination can also be used.

[2] A sufficient condition for $\mathcal{L}(X) \equiv X^{-1}(\mathcal{L})$ to exist is for $\mathcal{L}$ to be continuous and π to have a connected support. See Chopin and Robert (2010) and Feroz et al. (2013, Appendix C) for a more detailed measure-theoretic discussion.

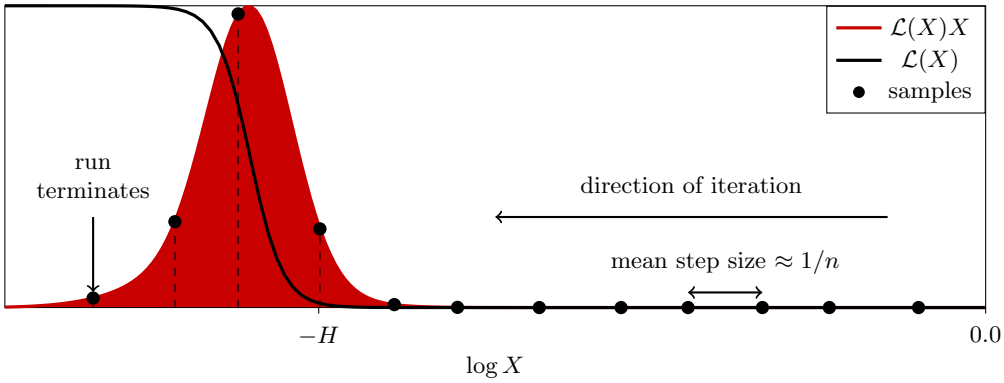

Figure 2: A schematic representation of standard nested sampling with a constant number of live points n. The curve $\mathcal{L}(X)X$ shows the relative posterior mass, the bulk of which is contained in some small fraction $\exp(-H)$ of the prior and is only visible on a log scale in X. The algorithm iterates inwards in X exponentially with stochastic shrinkage ratios distributed according to (5).

Evidence estimation

Nested sampling therefore allows one to approximate the evidence (4) via a quadrature sum over the dead points

$$\mathcal{Z}(\mathbf{t}) \approx \sum_{i \in \text{dead}} \mathcal{L}_i w_i(\mathbf{t}), \tag{6}$$

where $\mathbf{t} = \{t_1, t_2, \ldots, t_{n_{\text{dead}}}\}$ are the unknown set of shrinkage ratios for the n_{dead} iterations of the nested sampling process, and each t_i is an independent random variable drawn from distribution (5). The shrinkage ratios define the prior volumes via $X_i(\mathbf{t}) = \prod_{k=0}^{i} t_k$, and the w_i are appropriately chosen quadrature weights roughly corresponding to the volume of the "prior shell" to which a given dead point belongs. For example, using the trapezium rule: $w_i(\mathbf{t}) = \frac{1}{2}(X_{i-1}(\mathbf{t}) - X_{i+1}(\mathbf{t}))$. Given that the shrinkage ratios $\mathbf{t}$ are a priori unknown, one typically calculates an expected value and error on the evidence (6) using the distribution (5).

The dominant source of error in evidence estimates from perfect nested sampling is the statistical variation in the unknown volumes of the prior "shells" $w_i(\mathbf{t})$[3]. Skilling (2006) demonstrates that the uncertainty of $\log \mathcal{Z}$ is dominated by the Poisson variability in the number of steps required to reach the bulk of the posterior mass.

[3]The error from approximating the integral for $\mathcal{Z}$ with a sum can be safely neglected unless the number of live points n is very small; for example trapezium rule error goes as $\mathcal{O}(1/n^2)$. There is also some error from terminating the algorithm and truncating the sum, but this is can be made negligible with appropriate termination conditions.

Parameter estimation

One may also perform posterior inference from nested sampling by using the dead points to construct a set of posterior samples with weights proportional to their share of the posterior mass (Skilling, 2006):

$$p_i(\mathbf{t}) = \frac{w_i(\mathbf{t})\mathcal{L}_i}{\sum_i w_i(\mathbf{t})\mathcal{L}_i} = \frac{w_i(\mathbf{t})\mathcal{L}_i}{\mathcal{Z}(\mathbf{t})}. \tag{7}$$

As before, $\mathbf{t}$ is the set of prior shrinkage ratios with their stochasticity determined by (5), and in the trapezium rule case $w_i(\mathbf{t}) = \frac{1}{2}(X_{i-1}(\mathbf{t}) - X_{i+1}(\mathbf{t}))$. Nested sampling software packages such as MultiNest and PolyChord produce posterior files containing only the expected values $\mathrm{E}[p_i(\mathbf{t})]$.

The dominant sampling errors in estimating some parameter or function of parameters $f(\theta)$ from perfect nested sampling typically come from two sources:

(i) approximating the relative point weights $p_i(\mathbf{t})$ with their expectation $\mathrm{E}[p_i(\mathbf{t})]$ using (5);

(ii) approximating the mean value of a function of parameters over an entire iso-likelihood contour with its value at a single point $f(\theta_i)$.

For a detailed discussion of nested sampling parameter estimation and the sampling errors involved in the process see Higson et al. (2017).

Combining and dividing nested sampling runs

Skilling (2006) describes how several standard nested sampling runs $r = 1, 2, \ldots$ with constant live points $n^{(r)}$ may be combined simply by merging the dead points and sorting by likelihood value. The combined sequence of dead points is equivalent to a single nested sampling run with $n_{\text{combined}} = \sum_r n^{(r)}$ live points.

Higson et al. (2017) gives an algorithm for the reverse procedure — decomposing a nested sampling run with n live points into a set of n valid nested sampling runs, each with 1 live point. These single live point runs, which we term *threads*, are the smallest unit from which valid nested sampling runs can be constructed and will prove useful in developing dynamic nested sampling.

3 Variable numbers of live points

Before presenting our algorithm for dynamic nested sampling in Section 4, we first establish some basic results for a nested sampling run in which the number of live points varies.

Let us define n_i as the number of live points present for the prior shrinkage ratio t_i

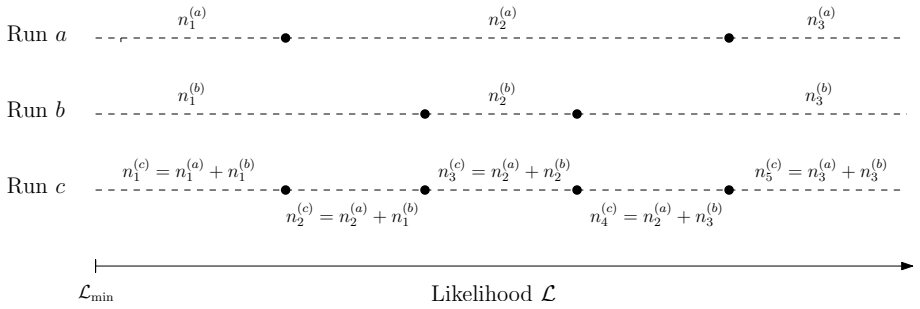

Figure 3: Combining nested sampling runs a and b with variable numbers of live points $\mathbf{n}^{(a)}$ and $\mathbf{n}^{(a)}$ into a single nested sampling run c; black dots show dead points arranged in order of increasing likelihood. The number of live points in run c at some likelihood equals the sum of the live points of run a and run b at that likelihood.

between dead points $i-1$ and i.[4]. In this notation all information about the number of live points for a nested sampling run can be expressed as a list of numbers $\mathbf{n} = \{n_1, n_2, \ldots, n_{n_{\text{dead}}}\}$ which correspond to the shrinkage ratios $\mathbf{t} = \{t_1, t_2, \ldots, t_{n_{\text{dead}}}\}$ Nested sampling calculations for variable numbers of live points differ from the constant live point case only in the use of different n_i in calculating the distribution of each t_i from (5).

Skilling (2006)'s method for combining constant live point runs, mentioned in Section 2, can be extended to accommodate variable numbers of live points by requiring that at any likelihood the live points of the combined run equals the sum of the live points of the constituent runs at that likelihood, as illustrated in Figure 3. Conversely if variable live point runs are divided into their constituent threads, some threads will start and finish part way through the run. On iso-likelihood contours when the number of live points is increased there is no longer a unique division into threads as there is for standard nested sampling.

In addition the variable live point framework provides a natural way to include the final set of live points remaining when a standard nested sampling run terminates in a calculation. These are uniformly distributed in the region of the prior with $\mathcal{L}(\theta) > \mathcal{L}_{\text{terminate}}$, and can be treated as samples from a dynamic nested sampling run with the number of live points reducing by 1 as each of the points remaining after termination is passed until the final point i has $n_i = 1$. This allows the final live points of standard nested sampling runs to be combined with variable live point runs.

The remainder of this section analyses the effects of local variations in the number of live points on the accuracy of nested sampling evidence calculation and parameter estimation. The dynamic nested sampling algorithm in Section 4 uses these results to allocate additional live points.

[4]In order for (5) to be valid, the number of live points must remain constant across the shrinkage ratios t_i between successive dead points. We therefore only allow the number of live points to change on iso-likelihood contours $\mathcal{L}(\theta) = \mathcal{L}_i$ where a dead point i is present. This restriction has negligible effects for typical calculations, and is automatically satisfied by most nested sampling implementations.

3.1 Effects on calculation accuracy

Nested sampling calculates the evidence $\mathcal{Z}$ as the sum of sample weights (6); the dominant sampling errors are from statistically estimating shrinkage ratios t_i which affect the weights of all subsequent points. In Section B of the supplementary material we show that the reduction in evidence errors achieved by taking additional samples to increase the local number of live points n_i is inversely proportional to n_i, and is approximately proportional to the evidence contained in subsequent points. This makes sense as the dominant evidence errors are from statistically estimating shrinkages t_i which affect all subsequent points $j \geq i$.

In nested sampling parameter estimation, sampling errors come both from taking a finite number of samples in any region of the prior and from the stochastic estimation of their normalised weights p_i from (7). For a typical calculation with a constant number of live points many samples are taken before reaching any significant posterior mass, as shown schematically in Figure 2. These provide points with negligible posterior weight, and also make little contribution to normalised weights of the other points.

Distribution (5) gives the expected separation between points in $\log X$ as $1/n_i$, which is approximately proportional to the posterior mass represented by each point. Hence increasing the number of live points near the posterior peak means points' posterior weights are more evenly spread. This can dramatically increase the information content (Shannon entropy of the samples)

$$H = \exp\left(-\sum_i p_i \log p_i\right), \tag{8}$$

while also improving the accuracy of the normalised weights p_i (7). The Shannon entropy (8) can be maximised by increasing the number of live points wherever the posterior weights $\mathcal{L}_i w_i$ are greatest.

When calculating the mean, variance or some other quantity for a parameter or function of parameters $f(\theta)$, the contribution of each sample i is dependent on $f(\theta_i)$ and therefore an optimum allocation of live points is different for different problems. In most cases the relative weight p_i of samples is a good approximation for their influence on a calculation, but for some problems a large contribution may come from a small region of the posterior mass with low likelihood but extreme parameter values such as the tails of the posterior distribution. Estimating the importance of points to a specific parameter estimation calculation is discussed in Section C of the supplementary material.

4 Dynamic nested sampling

We now present an algorithm for performing nested sampling calculations with a dynamically varying number of live points to optimise the allocation of samples.

Since the distribution of posterior mass as a function of the likelihood is a priori unknown, we first approximate it by performing a standard nested sampling run with

some small constant number of live points n_{init}. The algorithm then proceeds by iteratively calculating the range of likelihoods where increasing the number of live points will have the greatest effect on calculation accuracy, and generating an additional thread[5] running over these likelihoods.

From the discussion in Section 3 we define functions to measure the relative importance of a sample i for evidence calculation[6] and parameter estimation respectively as

$$I_{\mathcal{Z}}(i) \propto \frac{\mathrm{E}[\mathcal{Z}_{>i}]}{n_i}, \tag{9}$$

$$I_{\text{param}}(i) \propto \mathcal{L}_i w_i. \tag{10}$$

Modifying (10) to optimise for estimation of a specific parameter is discussed in Section C of the supplementary material.

The user specifies how to divide computational resources between evidence calculation and parameter estimation through an input goal $G \in [0, 1]$, where $G = 0$ corresponds to optimising for evidence calculation and $G = 1$ optimises for parameter estimation. The dynamic nested sampling algorithm calculates points' importance as a weighted sum

$$I(G, i) = (1 - G)\frac{I_{\mathcal{Z}}(i)}{\sum_j I_{\mathcal{Z}}(j)} + G\frac{I_{\text{param}}(i)}{\sum_j I_{\text{param}}(j)}. \tag{11}$$

The likelihood range in which to run an additional thread is chosen by finding all points with importance greater than some fraction (we use 90%) of the largest importance. To ensure any steep or discontinuous increases in the likelihood $\mathcal{L}(X)$ are captured we find the first point j and last point k which meet this condition, then generate an additional thread starting at $\mathcal{L}_{j-1}$ and ending when a point is sampled with likelihood greater than $\mathcal{L}_{k+1}$. If j is the first dead point, threads which initially sample the whole prior are generated. If k is the final dead point then the thread will stop when a sample with likelihood greater than $\mathcal{L}_k$ is found. This allows the new thread to continue beyond $\mathcal{L}_k$, meaning dynamic nested sampling iteratively explores higher likelihoods when this is the most effective use of samples.

Unlike in standard nested sampling, more accurate dynamic nested sampling results can be obtained simply by continuing the calculation for longer. The user must specify a condition at which to stop dynamically adding threads, such as when fixed number of samples has been taken or some desired level of accuracy has been achieved. Sampling errors on evidence and parameter estimation calculations can be estimated from the dead points at any stage using the method described in Higson et al. (2017). We term

[5] If required some n_{batch} additional threads can be generated at each step to reduce the number of importance calculations. We find in empirical tests that this has little effect on efficiency gains from dynamic nested sampling when the number of samples taken in each batch is small compared to the total number of samples in the run.

[6] Alternatively (9) can be replaced with a more complex expression using the result derived in Section B of the supplementary material (24), although we find this typically makes little difference to results.

these *dynamic termination conditions* to distinguish them from the type of termination conditions used in standard nested sampling.

More formally our dynamic nested sampling algorithm is:

Output : Samples and live points information **n**.
Input : Goal G, n_{init}, dynamic termination condition.

Generate a nested sampling run with a constant number of live points n_{init};
while *dynamic termination condition not satisfied* **do**
  recalculate importance $I(G, i)$ of all points;
  find first point j and last point k with importance of $> 90\%$ of the largest importance;
  generate a additional thread[5] starting at $\mathcal{L}_{j-1}$ and ending with the first sample taken with likelihood greater than $\mathcal{L}_{k+1}$;
end

Algorithm 1: Dynamic nested sampling.

5 Numerical tests

In the manner described by Keeton (2011), we perform empirical tests using spherically symmetric analytical cases where one can obtain uncorrelated samples from the prior space within some likelihood contour using standard techniques. We term this *perfect nested sampling*. Nested sampling software used for practical problems may cause additional effects from imperfect sampling within a likelihood contour that are specific to a given implementation — we discuss these in Section 6.

Perfect nested sampling calculations depend on the likelihood $\mathcal{L}(\theta)$ and prior $\pi(\theta)$ only through the distribution of posterior mass $\mathcal{L}(X)$ and the distribution of parameters on iso-likelihood contours $P(f(\theta)|X)$, both of which are functions of $\mathcal{L}(\theta)$ and $\pi(\theta)$ (Higson et al., 2017). We therefore empirically test our method using likelihoods and priors with a wide range of distributions of posterior mass, and consider several functions of parameters $f(\theta)$ in each case.

We first examine perfect nested sampling of d-dimensional spherical unit Gaussian likelihoods

$$\mathcal{L}(\theta) = (2\pi)^{-d/2} \mathrm{e}^{-|\theta|^2/2}, \tag{12}$$

with d-dimensional co-centred spherical Gaussian priors

$$\pi(\theta) = (2\pi\sigma_\pi^2)^{-d/2} \mathrm{e}^{-|\theta|^2/2\sigma_\pi^2}. \tag{13}$$

For additional tests using distributions with lighter and heavier tails than Gaussians we use d-dimensional exponential power likelihoods

$$\mathcal{L}(\theta) = \frac{d\,\Gamma(\frac{d}{2})}{\pi^{\frac{d}{2}} 2^{1+\frac{1}{2b}} \Gamma(1+\frac{n}{2b})} \mathrm{e}^{-|\theta|^{2b}/2}, \tag{14}$$

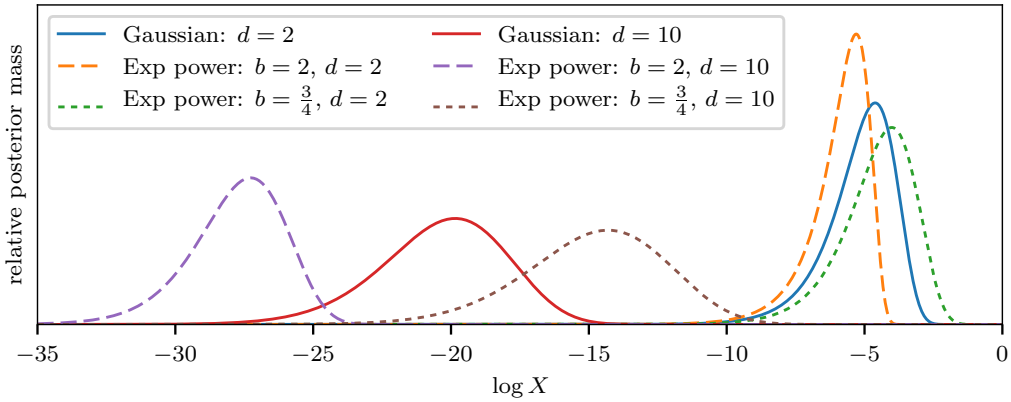

Figure 4: Relative posterior mass ($\propto \mathcal{L}(X)X$) as a function of $\log X$ for Gaussian likelihoods (12) and exponential power likelihoods (14) with $b = 2$ and $b = \frac{3}{4}$. Each has a Gaussian prior (13) with $\sigma_\pi = 10$. The lines are scaled so that the area under each of them is equal.

where $b = 1$ corresponds to a d-dimensional Gaussian (12). The different distributions of posterior mass in $\log X$ for (12) and (14) with dimensions d are illustrated in Figure 4.

In tests of parameter estimation we denote the first component of the θ vector as $\theta_{\hat{1}}$, although by symmetry the results will be the same for any component. $\overline{\theta_{\hat{1}}}$ is the mean of the posterior distribution of $\theta_{\hat{1}}$, and the one-tailed $Y\%$ upper credible interval $\text{C.I.}_{Y\%}(\overline{\theta_{\hat{1}}})$ is the value $\theta^*_{\hat{1}}$ for which $P(\theta_{\hat{1}} < \theta^*_{\hat{1}}|\mathcal{L}, \pi) = Y/100$.

Tests of dynamic nested sampling use $n_{\text{init}} = 5$ and terminate after a fixed number of samples, which is set such that they use similar or slightly fewer samples than standard nested sampling runs we comare them to. Standard nested sampling runs use the termination conditions described by Handley et al. (2015b, Section 3.4), stopping when the estimated evidence contained in the live points is less than 10^{-4} times the evidence contained in dead points.

We begin by testing dynamic nested sampling on a 10-dimensional Gaussian likelihood (12) with a Gaussian prior (12) and $\sigma_\pi = 10$. Figure 5 shows the relative allocation of live points as a function of $\log X$ for standard and dynamic nested sampling runs. The dynamic nested sampling algorithm (Algorithm 1) can accurately and consistently allocate live points, as can be seen by comparison with the analytically calculated distribution of posterior mass and posterior mass remaining[7]. Similar diagrams for expo-

[7]Dynamic nested sampling live point allocations do not precisely match the distribution of posterior mass and posterior mass remaining in the $G = 1$ and $G = 0$ cases because they include the initial exploratory run with a constant n_{init} live points, and because each thread includes one sample taken after its termination condition is met. Furthermore as additional live points are added where samples' importance is more than 90% of the maximum importance, the number of live points allocated by dynamic nested sampling is approximately constant for regions with importance of greater than ~90% of the maximum — this can be clearly seen in Figure 5 near the peak number of live points in the $G = 1$ case.

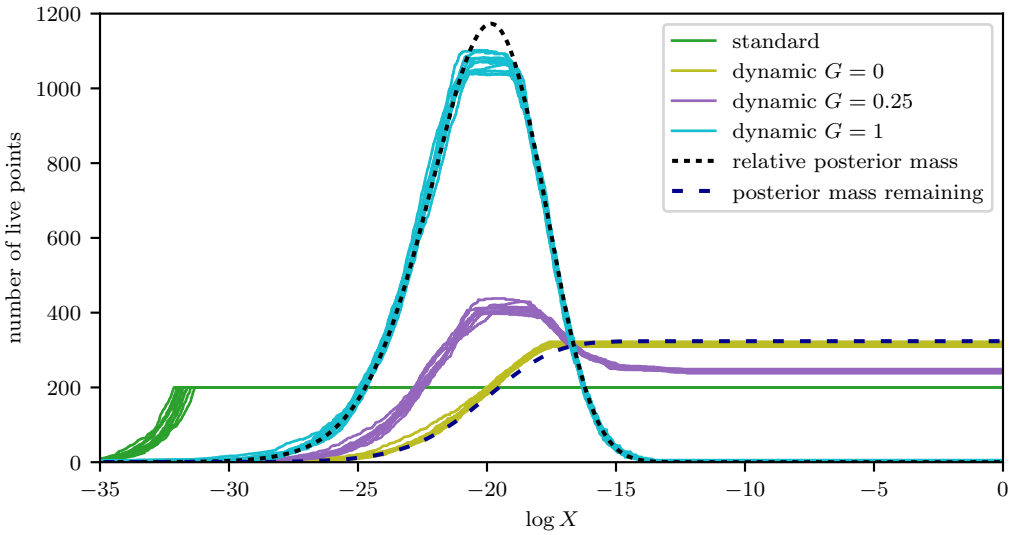

Figure 5: Live point allocation for a 10-dimensional Gaussian likelihood (12) with a Gaussian prior (13) and $\sigma_\pi = 10$. Solid lines show the number of live points as a function of $\log X$ for 10 standard nested sampling runs, and 10 dynamic nested sampling runs with a similar number of samples and different values of G. The dotted and dashed lines show the relative posterior mass $\propto \mathcal{L}(X)X$ and the posterior mass remaining $\propto \int_{-\infty}^{X} \mathcal{L}(X')X' \,\mathrm{d}X'$ at each point in $\log X$; for comparison these lines are scaled to have the same area under them as the average of the number of live point lines. Standard runs include the final set of live points at termination, which are modeled using a decreasing number of live points as discussed in Section 3. Similar diagrams for exponential power likelihoods (14) with $b = 2$ and $b = \frac{3}{4}$ are presented in Section A of the supplementary material (Figures 9 and 10).

nential power likelihoods (14) with $b = 2$ and $b = \frac{3}{4}$ are presented in Section A of the supplementary material (Figures 9 and 10), and show the allocation of live points is also accurate in these cases.

The distribution of results from repeated standard and dynamic nested sampling calculations with a similar number of samples is shown in Table 1 and Figure 6. Dynamic nested sampling optimised for evidence calculation ($G = 0$) and at parameter estimation ($G = 1$) produce significantly more accurate results than standard nested sampling. In addition results for dynamic nested sampling with $G = 0.25$ show that both evidence calculation and parameter estimation accuracy can be improved simultaneously. Equivalent results tables for 10-dimensional exponential power likelihoods (14) with $b = 2$ and $b = \frac{3}{4}$ are presented in Section A of the supplementary material (Tables 2 and 3).

As nested sampling calculation errors are typically proportional to the square root of the computational effort applied (Skilling, 2006; Higson et al., 2017), the increase in

	# samples	$\log \mathcal{Z}$	$\overline{\theta_{\hat{1}}}$	C.I.$_{84\%}(\overline{\theta_{\hat{1}}})$
St.Dev. standard	6,583	0.298(5)	0.025(0.4)	0.041(0.6)
St.Dev. $G = 0$	6,515	0.247(4)	0.028(0.4)	0.045(0.7)
St.Dev. $G = 0.25$	6,509	0.269(4)	0.019(0.3)	0.031(0.5)
St.Dev. $G = 1$	6,494	1.72(3)	0.012(0.2)	0.020(0.3)
efficiency gain $G = 0$		1.5(1)	0.84(4)	0.83(4)
efficiency gain $G = 0.25$		1.2(1)	1.8(1)	1.8(1)
efficiency gain $G = 1$		0.030(1)	4.2(2)	4.3(2)

Table 1: Test of dynamic nested sampling for a 10-dimensional Gaussian likelihood (12) and a Gaussian prior (13) with $\sigma_\pi = 10$. The first four rows show the standard deviation of 2,000 calculations for standard nested sampling, dynamic nested sampling optimised purely for evidence calculation ($G = 0$), for both evidence and parameter estimation ($G = 0.25$) and purely for parameter estimation ($G = 1$). The final three rows show the computational efficiency gain (15) from dynamic nested sampling over standard nested sampling in each case. The first column shows the mean number of samples for the 2,000 runs; the remaining columns show calculations of the log evidence and the mean and 84% one-tailed credible interval of a parameter $\theta_{\hat{1}}$. Numbers in brackets show the error on the final digit.

efficiency (computational speedup) from dynamic nested sampling over standard nested sampling can be estimated as

$$\text{efficiency gain} = \frac{\text{Var}\left[\text{dynamic nested sampling calculation results}\right]}{\text{Var}\left[\text{standard nested sampling calculation results}\right]}, \tag{15}$$

where the calculation results from dynamic and standard nested sampling use approximately the same number of samples. The reduction in evidence errors for $G = 0$ and parameter estimation errors for $G = 1$ in Table 1 correspond to increasing efficiency by factors of approximately 1.5 and 4 respectively.

5.1 Efficiency gains for different distributions of posterior mass

Efficiency gains (15) from dynamic nested sampling depend on the fraction of the $\log X$ range explored which makes a significant contribution to calculation accuracy — if this is small then most samples taken by standard nested sampling contain little information and dynamic nested sampling can greatly improve performance. For parameter estimation ($G = 1$), only $\log X$ regions containing significant posterior mass ($\propto \mathcal{L}(X)X$) are important, whereas for evidence calculation ($G = 0$) all samples taken before the bulk of the posterior is reached are valuable. Both cases benefit from dynamic nested sampling using fewer samples to explore the region after most of the posterior mass has been passed but before termination.

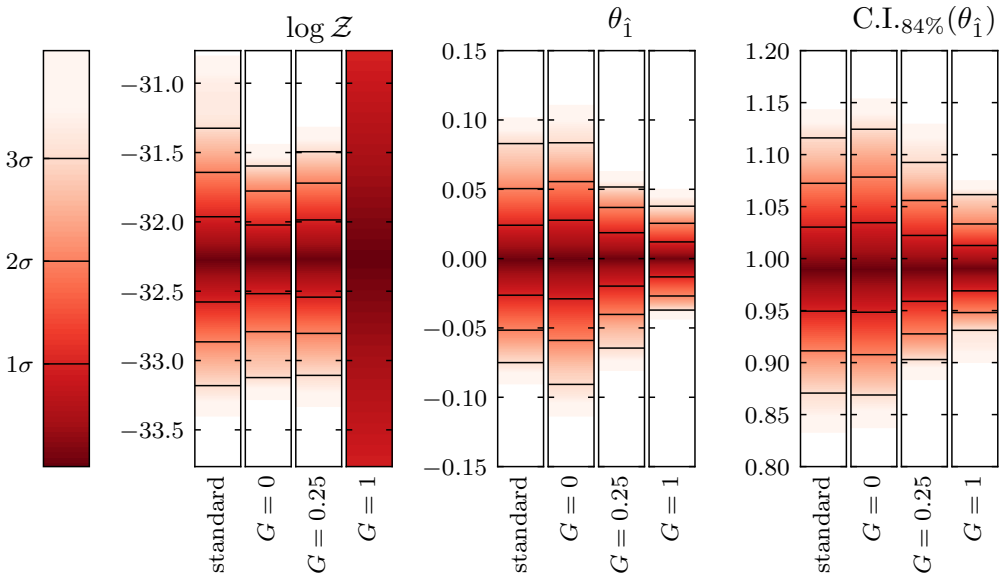

Figure 6: Distributions of results for the standard nested sampling and dynamic nested sampling calculations in Table 1. Dynamic nested sampling with $G = 0$ and $G = 1$ significantly reduces evidence and parameter estimation sampling errors respectively compared to standard nested sampling. Dynamic nested with $G = 0.25$ reduces both evidence and parameter estimation sampling errors. The colour scale shows the fraction of the cumulative probability distribution lying between some region and the median.

We now test the efficiency gains (15) of dynamic nested sampling empirically for a wide range of distributions of posterior mass by considering Gaussian likelihoods (12) and exponential power likelihoods (14) of different dimensions d and prior sizes σ_π. The results are presented in Figures 7 and 8, and show large efficiency gains from dynamic nested sampling for parameter estimation in all of these cases.

Increasing the dimension d typically means the posterior mass is contained in a smaller fraction of the prior volume (Higson et al., 2017), as can be seen in Figure 4. In the spherically symmetric cases we consider the range of $\log X$ to be explored before significant posterior mass is reached increases approximately linearly with d. This increases the efficiency gain (15) from dynamic nested sampling for parameter estimation ($G = 1$) but reduces it for evidence calculation ($G = 0$). High dimensional problems often have the vast majority of the $\log X$ range explored lying before any significant posterior mass is reached; this results in very large efficiency gains for parameter estimation but almost no gains for evidence calculation as shown in Figure 7. For the 1000-dimensional exponential power likelihood with $b = 2$, dynamic nested sampling with $G = 1$ improves parameter estimation efficiency by a factor of up to 67 ± 4.

Increasing the size of the prior σ_π increases the fraction of the $\log X$ range explored before any significant posterior mass is reached, resulting in larger efficiency gains (15)

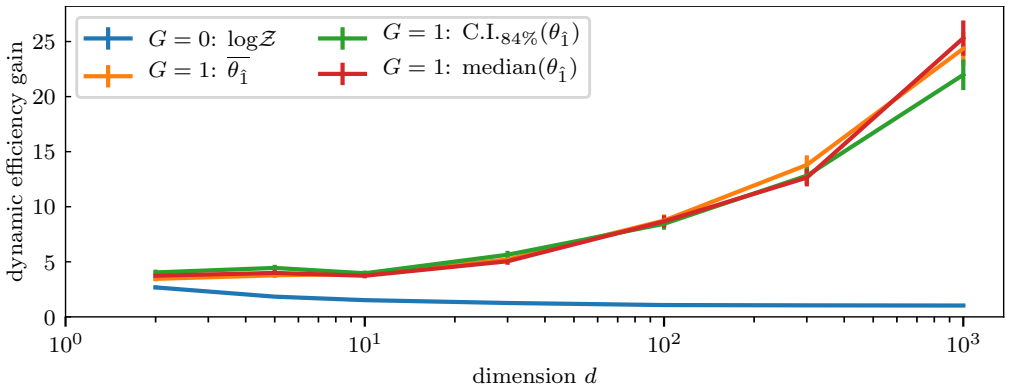

(a) Efficiency gain (15) for Gaussian likelihoods (12).

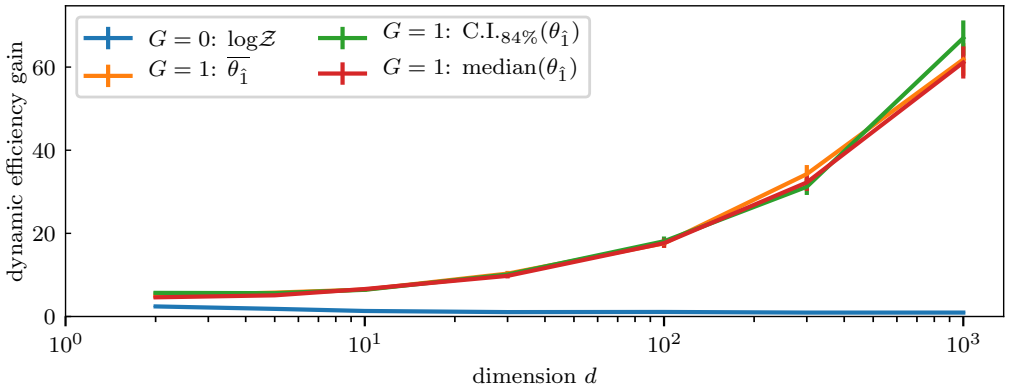

(b) Efficiency gain (15) for exponential power likelihoods (14) with $b = 2$.

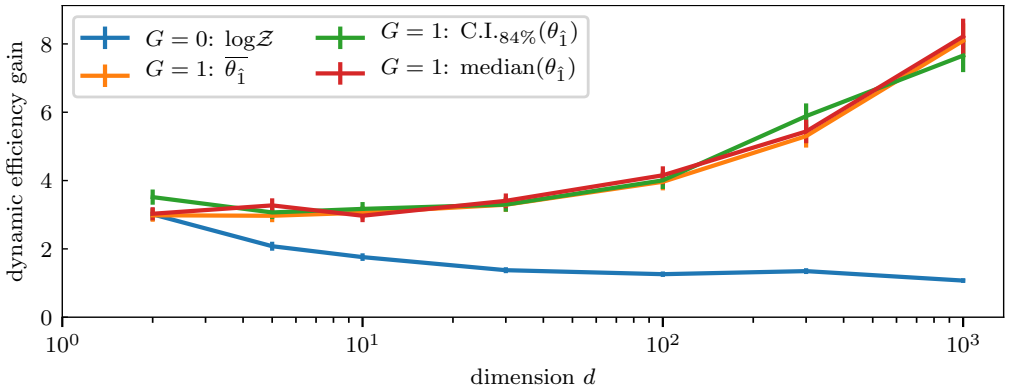

(c) Efficiency gain (15) for exponential power likelihoods (14) with $b = \frac{3}{4}$.

Figure 7: Efficiency gain (15) from dynamic nested sampling compared to standard nested sampling for likelihoods of different dimensions; each has a Gaussian prior (13) with $\sigma_\pi = 10$. Results are shown for calculations of the log evidence and the mean, median and 84% one-tailed credible interval of a parameter $\theta_{\hat{1}}$. Each efficiency gain is calculated using 1000 standard nested sampling calculations with $n = 100$ and 1000 dynamic nested sampling calculations using a similar or slightly smaller number of samples.

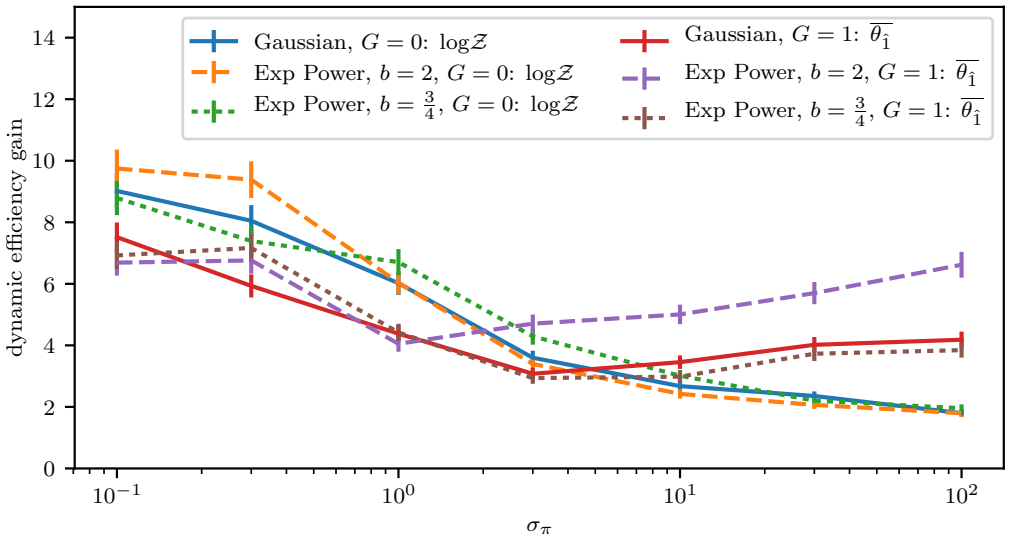
Gaussian, $G = 0$: $\log \mathcal{Z}$
Exp Power, $b = 2$, $G = 0$: $\log \mathcal{Z}$
Exp Power, $b = \frac{3}{4}$, $G = 0$: $\log \mathcal{Z}$
Gaussian, $G = 1$: $\overline{\theta_{\hat{1}}}$
Exp Power, $b = 2$, $G = 1$: $\overline{\theta_{\hat{1}}}$
Exp Power, $b = \frac{3}{4}$, $G = 1$: $\overline{\theta_{\hat{1}}}$
dynamic efficiency gain
σ_π

Figure 8: Efficiency gain (15) from dynamic nested sampling for Gaussian priors (13) of different sizes σ_π. Results are shown for calculations of the log evidence and the mean of a parameter $\theta_{\hat{1}}$ for 2-dimensional Gaussian likelihoods (12) and 2-dimensional exponential power likelihoods (14) with $b = 2$ and $b = \frac{3}{4}$. Each efficiency gain is calculated using 1000 standard nested sampling calculations with $n = 100$ and 1000 dynamic nested sampling calculations using a similar or slightly smaller number of samples.

from dynamic nested sampling for parameter estimation ($G = 1$) but smaller gains for evidence calculation ($G = 0$). However when σ_π is small the bulk of the posterior mass is reached after a small number of steps, and most of the $\log X$ range explored is after the majority of the posterior mass but before termination. Dynamic nested sampling places few samples in this region, leading to large efficiency gains for both parameter estimation and evidence calculation, as shown in Figure 8. When $\sigma_\pi = 0.1$, dynamic nested sampling evidence calculations with $G = 0$ improve efficiency over standard nested sampling by a factor of approximately 9.

6 Dynamic nested sampling with existing nested sampling software

Existing standard nested sampling software such as MultiNest and PolyChord can be easily adapted to perform dynamic nested sampling. We are working on incorporating dynamic nested sampling into PolyChord 2, which is currently in production. PolyChord 2 will be able to perform nested sampling in up to approximately 1000 dimensions — dynamic nested sampling can offer significant efficiency gains in such calculations.

We anticipate reloading a past iteration i of a PolyChord 2 nested sampling run in order to add additional threads will be less computationally expensive than a single likelihood call for many problems. Nevertheless it may prove most efficient for nested sampling software performing dynamic nested sampling to generate additional threads in selected likelihood regions in batches rather than one at a time; provided the number of samples taken in each batch is much less that the total number of samples in the run this will have little effect on efficiency gains from dynamic nested sampling.

Nested sampling software used for practical problems can only approximately sample randomly from the prior within iso-likelihood contours — this introduces additional implementation-specific errors which are not present in perfect nested sampling. The most important concern for dynamic nested sampling is ensuring no modes or other regions of significant posterior mass are lost. Dynamic nested sampling aids the location of modes which become separated from the remainder of the posterior at likelihood values where it places more samples than standard nested sampling. If modes separate at likelihood values where dynamic nested sampling assigns few samples, n_{init} must be made large enough to ensure no significant modes are lost. However even if some significant fraction of the computational budget f is used for the initial exploration with n_{init} live points, efficiency gains will be at least $(1 - f)$ times what could be achieved with a very small n_{init}. MultiNest and PolyChord use dead points to help them sample within iso-likelihood contours, so provided no significant modes are lost we expect the additional samples from dynamic nested sampling in the regions of $\log X$ of most importance to the calculation will reduce implementation-specific errors.

7 Conclusion

This paper began with an analysis of the effects of changing the number of live points on the accuracy of nested sampling parameter estimation and evidence calculations. We then presented dynamic nested sampling (Algorithm 1), which varies the number of live points to allocate posterior samples efficiently for a priori unknown likelihoods and priors.

Dynamic nested sampling can be optimised specifically for parameter estimation or evidence calculation, showing increases in computational efficiency over standard nested sampling (15) by factors of up to ~67 and ~9 respectively in numerical tests. Furthermore parameter estimation and evidence calculation accuracy can both be improved simultaneously. We discussed factors effecting the efficiency gain from dynamic nested sampling, including showing large improvements in parameter estimation are possible when the posterior mass is contained in a small region of the prior (as is often the case in high dimensional problems). Empirical tests show significant efficiency gains from dynamic nested sampling for a wide range likelihoods, priors, dimensions and estimators considered. Another advantage of dynamic nested sampling is that more accurate results can be obtained by continuing the run for longer, unlike in standard nested sampling.

Dynamic nested sampling can be easily incorporated in existing standard nested sampling software; we are currently working on including it in the forthcoming PolyChord 2 software package.

References

Brewer, B. J., Pártay, L. B., and Csányi, G. (2011). "Diffusive nested sampling." *Statistics and Computing*, 21(4): 649–656. 2

Chopin, N. and Robert, C. P. (2010). "Properties of nested sampling." *Biometrika*, 97(3): 741–755. 3

Feroz, F. and Hobson, M. P. (2008). "Multimodal nested sampling: An efficient and robust alternative to Markov Chain Monte Carlo methods for astronomical data analyses." *Monthly Notices of the Royal Astronomical Society*, 384(2): 449–463. 1

Feroz, F., Hobson, M. P., and Bridges, M. (2009). "MultiNest: An efficient and robust Bayesian inference tool for cosmology and particle physics." *Monthly Notices of the Royal Astronomical Society*, 398(4): 1601–1614. 1

Feroz, F., Hobson, M. P., Cameron, E., and Pettitt, A. N. (2013). "Importance Nested Sampling and the MultiNest Algorithm." *preprint (arXiv:1306.2144)*. 1, 3

Handley, W. J., Hobson, M. P., and Lasenby, A. N. (2015a). "PolyChord: Nested sampling for cosmology." *Monthly Notices of the Royal Astronomical Society: Letters*, 450(1): L61–L65. 1

— (2015b). "PolyChord: next-generation nested sampling." *Monthly Notices of the Royal Astronomical Society*, 15: 1–15. 1, 10

Higson, E., Handley, W., Hobson, M., and Lasenby, A. (2017). "Sampling errors in nested sampling parameter estimation." *preprint (arXiv:1703.09701)*. 2, 5, 8, 9, 11, 13

Keeton, C. R. (2011). "On statistical uncertainty in nested sampling." *Monthly Notices of the Royal Astronomical Society*, 414(2): 1418–1426. 2, 9

Martiniani, S., Stevenson, J. D., Wales, D. J., and Frenkel, D. (2014). "Superposition enhanced nested sampling." *Physical Review X*, 4(3). 2

Planck Collaboration (2016). "Planck 2015. XX. Constraints on inflation." *Astronomy & Astrophysics*, 594: A20. 1

Skilling, J. (2006). "Nested sampling for general Bayesian computation." *Bayesian Analysis*, 1(4): 833–860. 1, 2, 3, 4, 5, 6, 11

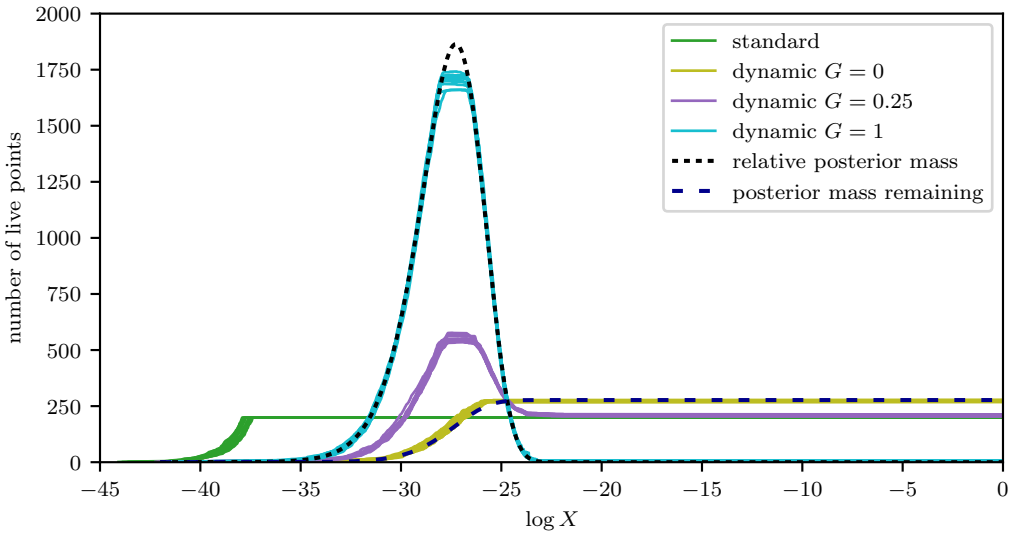

Figure 9: As in Figure 5 but with a 10-dimensional exponential power likelihood (14) with $b = 2$, and a Gaussian prior (13) with $\sigma_\pi = 10$.

Supplementary material

A Additional numerical tests

This section contains additional tests of dynamic nested sampling using 10-dimensional exponential power likelihoods (14) with $b = 2$ and $b = \frac{3}{4}$; compared to Gaussians (12) these respectively have lighter and heavier tails. Each uses a Gaussian prior (12) with $\sigma_\pi = 10$. Figures 9 and 10 show that the dynamic nested sampling algorithm can accurately and consistently allocate live points for these likelihoods.

Tables 2 and 3 show the errors in repeated calculations for standard and dynamic nested sampling in these two cases. The reduction in errors correspond to increasing efficiency of evidence calculation ($G = 0$) and parameter estimation ($G = 1$) by factors of up 1.5 ± 0.1 and 6.6 ± 0.3 respectively in the $b = 2$ case, and by factors of up to 1.7 ± 0.1 and 3.1 ± 1 in the $b = \frac{3}{4}$ case.

B Effect of varying n on evidence calculation accuracy

Nested sampling estimates the evidence as the expectation of (6), with the dominant sampling errors from the unknown shrinkage ratios t_i which are independently distributed according to (5). We now investigate the effect of increasing the number of live points n_i across some shrinkage t_i by considering (6) with all $t_{j\neq i}$ marginalised out and

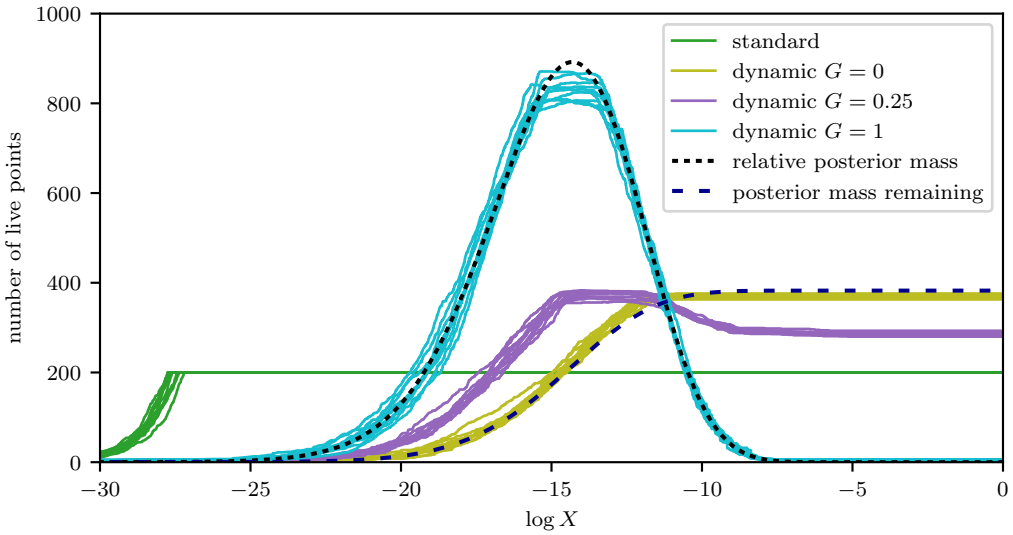

Figure 10: As in Figure 5 but with a 10-dimensional exponential power likelihood (14) with $b = \frac{3}{4}$, and a Gaussian prior (13) with $\sigma_\pi = 10$.

	# samples	$\log \mathcal{Z}$	$\overline{\theta_{\hat{1}}}$	C.I.$_{84\%}(\overline{\theta_{\hat{1}}})$
St.Dev. standard	7,711	0.368(6)	0.014(0.2)	0.021(0.3)
St.Dev. $G = 0$	7,727	0.304(5)	0.016(0.3)	0.026(0.4)
St.Dev. $G = 0.25$	7,722	0.356(6)	$0.865(14) \cdot 10^{-2}$	0.013(0.2)
St.Dev. $G = 1$	7,717	2.20(4)	$0.527(8) \cdot 10^{-2}$	$0.829(13) \cdot 10^{-2}$
efficiency gain $G = 0$		1.5(1)	0.68(3)	0.65(3)
efficiency gain $G = 0.25$		1.1(1)	2.4(1)	2.5(1)
efficiency gain $G = 1$		0.028(1)	6.6(3)	6.3(3)

Table 2: As in Table 1 but with a 10-dimensional exponential power likelihood (14) with $b = 2$, and a Gaussian prior (13) with $\sigma_\pi = 10$.

conditioned on t_i, defining

$$\mathcal{Z}(t_i) \equiv \int \left(\sum_j w_j \mathcal{L}_j \right) \prod_{j \neq i} P(t_j) \, \mathrm{d}t_j. \tag{16}$$

For simplicity instead of using the trapezium rule we calculate point weight as $w_i = X_{i-1} - X_i = (1 - t_i) \prod_{k<i} t_k$. In this case uncertainty in t_i causes sampling errors in

	# samples	$\log \mathcal{Z}$	$\overline{\theta_{\hat{1}}}$	C.I.$_{84\%}(\overline{\theta_{\hat{1}}})$
St.Dev. standard	5,679	0.246(4)	0.041(0.7)	0.069(1)
St.Dev. $G = 0$	5,645	0.189(3)	0.044(0.7)	0.073(1)
St.Dev. $G = 0.25$	5,645	0.201(3)	0.032(0.5)	0.054(0.9)
St.Dev. $G = 1$	5,633	1.31(2)	0.024(0.4)	0.039(0.6)
efficiency gain $G = 0$		1.7(1)	0.89(4)	0.89(4)
efficiency gain $G = 0.25$		1.5(1)	1.7(1)	1.6(1)
efficiency gain $G = 1$		0.035(2)	2.9(1)	3.1(1)

Table 3: As in Table 1 but with a 10-dimensional exponential power likelihood (14) with $b = \frac{3}{4}$, and a Gaussian prior (13) with $\sigma_\pi = 10$.

the weight of point i and all subsequent points[8] and

$$\sum_j w_j(\mathbf{t})\mathcal{L}_j = \left[\sum_{j<i} w_j\mathcal{L}_j\right] + (1-t_i)\left[\frac{w_i\mathcal{L}_i}{1-t_i}\right] + t_i\left[\sum_{j>i}\frac{w_j\mathcal{L}_j}{t_i}\right], \tag{17}$$

where the terms in square brackets are independent of t_i. Substituting (17) into (16) and integrating gives

$$\mathcal{Z}(t_i) \quad = \quad \mathrm{E}[\mathcal{Z}_{<i}] + (1-t_i)\frac{\mathrm{E}[\mathcal{L}_i w_i]}{(1-\mathrm{E}[t_i])} + t_i\frac{\mathrm{E}[\mathcal{Z}_{>i}]}{\mathrm{E}[t_i]}, \tag{18}$$

where we have defined $\mathcal{Z}_{>i} \equiv \sum_{k>i}\mathcal{L}_k w_k$ and $\mathcal{Z}_{<i} \equiv \sum_{k<i}\mathcal{L}_k w_k$. From the distribution of the shrinkage ratios (5)

$$\mathrm{E}[t_i] = \frac{n_i}{1+n_i}, \qquad \text{St.Dev.}[t_i] = \frac{{n_i}^{1/2}}{(n_i+1)(n_i+2)^{1/2}}, \tag{19}$$

so (18) can be written

$$\mathcal{Z}(t_i) = \Big(\mathrm{E}[\mathcal{Z}_{<i}] + \mathrm{E}[\mathcal{L}_i w_i](n_i+1)\Big) + t_i\left(\frac{n_i}{n_i+1}\mathrm{E}[\mathcal{Z}_{>i}] - (1+n_i)\mathrm{E}[\mathcal{L}_i w_i]\right), \tag{20}$$

where terms in large brackets are independent of t_i. Using the expression for St.Dev.$[t_i]$ from (19), the standard deviation of $\mathcal{Z}(t_i)$ is

$$\text{St.Dev.}[\mathcal{Z}(t_i)] = \frac{n_i^{3/2}}{(n_i+2)^{1/2}(n_i+1)^2}\mathrm{E}[\mathcal{Z}_{>i}] - \frac{n_i^{1/2}}{(n_i+2)^{1/2}}\mathrm{E}[\mathcal{L}_i w_i], \tag{21}$$

The expected number of samples (computational work) needed to increase the number of live points over some interval $(\mathcal{L}_a, \mathcal{L}_b)$ is proportional to the log prior shrinkage

[8] If the trapezium rule is used t_i also affects the weight of the previous point $i-1$, but this has little effect on the results.

$\log X(\mathcal{L}_a) - \log X(\mathcal{L}_b)$. Hence the expected extra samples ΔN_s required to increase the local number of live points n_i is proportional to the interval $\log t_i$, which has an expected size of $1/n_i$. The change in the error on the evidence with extra samples is therefore

$$\begin{aligned}
\frac{\mathrm{d}}{\mathrm{d}N_\mathrm{s}}\mathrm{St.Dev.}[\mathcal{Z}(t_i)] &= \frac{\mathrm{d}n_i}{\mathrm{d}N_\mathrm{s}}\frac{\mathrm{d}}{\mathrm{d}n_i}\mathrm{St.Dev.}[\mathcal{Z}(t_i)] && (22)\\
&\propto n_i \frac{\mathrm{d}}{\mathrm{d}n_i}\mathrm{St.Dev.}[\mathcal{Z}(t_i)] && (23)\\
&\propto -\frac{n_i^{3/2}(n_i^2-3)}{(n_i+1)^3(n_i+2)^{3/2}}\mathrm{E}[\mathcal{Z}_{>i}] - \frac{n_i^{1/2}}{(n_i+2)^{3/2}}\mathrm{E}[\mathcal{L}_i w_i]. && (24)
\end{aligned}$$

This quantity can be easily calculated for a set of dead points with little computational cost. Typically $n_i \gg 2$ and $\mathrm{E}[\mathcal{L}_i w_i] \ll \mathrm{E}[\mathcal{Z}_{>i}]$, in which case

$$\frac{\mathrm{d}}{\mathrm{d}N_\mathrm{s}}\mathrm{St.Dev.}[\mathcal{Z}(t_i)] \propto -\frac{\mathrm{E}[\mathcal{Z}_{>i}]}{n_i}. \tag{25}$$

Thus the accuracy gained from taking additional samples is approximately proportional to the evidence contained in subsequent dead points. This makes sense as the dominant evidence errors are from statistically estimating shrinkages t_i which affect all subsequent points $j \geq i$.

C Tuning for a specific parameter estimation problem

Dynamic nested sampling improves parameter estimation efficiency by placing more samples in $\log X$ regions with significant posterior mass and fewer in regions with little posterior mass. However for some likelihoods and parameter estimation problems a large contribution may come from samples in $\log X$ regions containing extreme parameter values but little posterior weight. In this case the expression for sample importances (10) can be modified to favour points with parameter values which will have a large effect on the calculation.

For example estimating the mean of some parameter or function of parameters $\mathrm{E}[f(\theta)] = \sum_i f(\theta_i)\mathcal{L}_i w_i$, one could calculate sample importances as

$$I_\mathrm{param}(i) \propto |f(\theta_i) - \mathrm{E}[f(\theta)]|\,\mathcal{L}_i w_i. \tag{26}$$

This expression is highly variable as each point i is a single sample from an iso-likelihood contour $\mathcal{L}(\theta) = \mathcal{L}_i$ which may cover a wide range of parameters. However dynamic nested sampling (Algorithm 1) uses only the first and last points of high importance in allocating new threads, so their placement is still accurate. For tuning dynamic nested sampling for calculating the mean of a parameter $\theta_{\hat{1}}$, (26) becomes

$$I_\mathrm{param}(i) \propto \left|\theta_{\hat{1}\,i} - \overline{\theta_{\hat{1}}}\right| \mathcal{L}_i w_i. \tag{27}$$

We illustrate tuning for a specific parameter by using dynamic nested sampling with a d-dimensional spherical unit Cauchy likelihood

$$\mathcal{L}(\theta) = \frac{\Gamma\left(\frac{1+d}{2}\right)}{\pi^{(d+1)/2}}\left(1 + |\theta|^2\right)^{-\left(\frac{d+1}{2}\right)}. \tag{28}$$

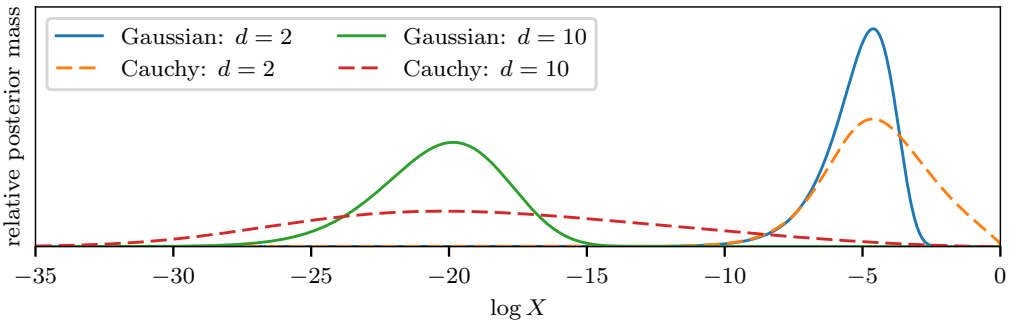

Figure 11: Relative posterior mass ($\propto \mathcal{L}(X)X$) as a function of $\log X$ for Cauchy likelihoods (28), with Gaussian likelihoods (12) shown for comparison. Each has a Gaussian prior (13) with $\sigma_\pi = 10$. The lines are scaled so that the area under each of them is equal.

The Cauchy likelihoods have extremely heavy tails (except in high dimensions) have significant posterior mass present across almost the entire range of $\log X$ explored, as shown in Figure 11. We therefore expect relatively low efficiency gains for dynamic parameter estimation ($G = 1$) in this case, but use it for a proof of principle.

Figure 12 shows the allocation of live points by dynamic nested sampling with and without tuning. In the tuned case the live points allocation is consistent with the analytical expectation of (27)[9], showing live points can be allocated correctly.

Table 4 shows the efficiency gain for dynamic nested sampling for a 10-dimensional Cauchy likelihood (28) with a Gaussian prior (13) and $\sigma_\pi = 10$. When estimating $\overline{\theta_{\hat{1}}}$ the calculation is dominated by samples in the tails of the distribution at low likelihoods and dynamic nested sampling therefore gives only a small efficiency gain (15) over standard nested sampling. Tuned dynamic nested sampling is able to improve efficiency gain, as shown in the final row of Table 4. Using the tuned importance function affects the performance gain for other calculations — in this case it slightly improves evidence estimates in comparison to the $G = 1$ case without tuning.

[9]For a Cauchy likelihood (28) with a co-centred spherically symmetric uniform prior, the analytic value of $\mathrm{E}[\theta_{\hat{1}}]$ is 0 and each iso-likelihood contour $\mathcal{L}(\theta) = \mathcal{L}(X)$ is a spherically symmetric surface with radius $|\theta|$. The expectation of $|\theta_i|$ on such an iso-likelihood contour is $|\theta|/\sqrt{d}$, so the analytical expectation of the importance (27) is

$$I_{\mathrm{param}}(X) \propto |\theta| X \mathcal{L}(X)/\sqrt{d}. \tag{29}$$

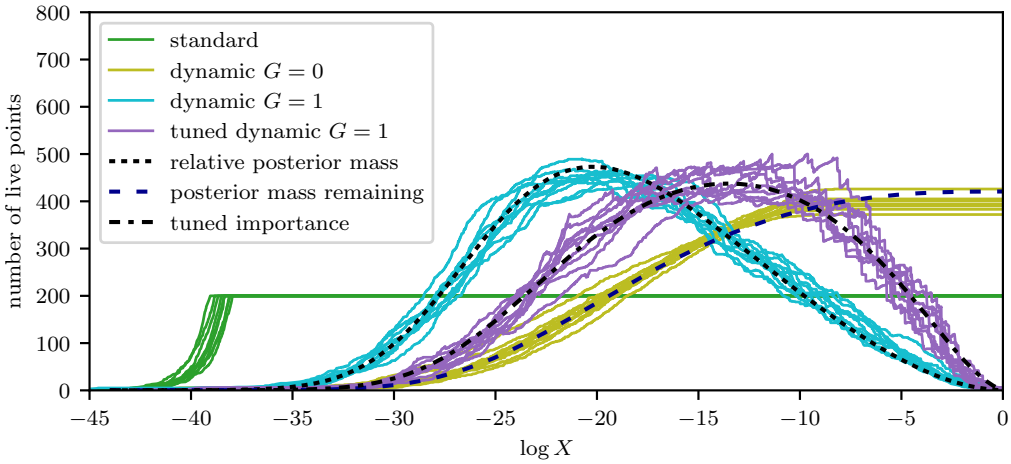

Figure 12: Live point allocation for a 10-dimensional Cauchy likelihood (28) with a Gaussian prior (13) and $\sigma_\pi = 10$. Solid lines show the number of live points as a function of $\log X$ for 10 standard nested sampling runs and 10 dynamic nested sampling runs with a similar number of samples and $G = 0$, $G = 1$ and with a tuned importance function (27) and $G = 1$. The dotted and dashed lines show the relative posterior mass $\propto \mathcal{L}(X)X$, the posterior mass remaining $\propto \int_{-\infty}^{X} \mathcal{L}(X')X' \, \mathrm{d}X'$ and the analytical expectation of the tuned importance function (27), which is given by (29)[9]. For comparison these lines are scaled to have the same area under them as the average of the number of live point lines.

	# samples	$\log \mathcal{Z}$	$\overline{\theta_{\hat{1}}}$	C.I.$_{84\%}(\overline{\theta_{\hat{1}}})$
St.Dev. standard	7,882	0.267(4)	0.021(0.3)	0.090(1)
St.Dev. $G = 0$	7,889	0.201(3)	0.018(0.3)	0.088(1)
St.Dev. $G = 1$	7,878	0.605(10)	0.019(0.3)	0.068(1)
St.Dev. $G = 1$ tuned	7,882	0.477(8)	0.016(0.3)	0.070(1)
efficiency gain $G = 0$		1.8(1)	1.3(1)	1.06(5)
efficiency gain $G = 1$		0.19(1)	1.2(1)	1.7(1)
efficiency gain $G = 1$ tuned		0.31(1)	1.6(1)	1.7(1)

Table 4: Test of tuned dynamic nested sampling with a 10-dimensional Cauchy likelihood (28), and a Gaussian prior (13) with $\sigma_\pi = 10$. The first four rows show the standard deviation of 2,000 calculations for standard nested sampling and dynamic nested sampling with $G = 0$, $G = 1$ and with a tuned importance function (27) and $G = 1$. The final three rows show the computational efficiency gain (15) from dynamic nested sampling over standard nested sampling in each case. The first column shows the mean number of samples for the 2,000 runs; the remaining columns show calculations of the log evidence and the mean and 84% one-tailed credible interval of a parameter $\theta_{\hat{1}}$. Numbers in brackets show the error on the final digit.